Study of Forced Convection Heat Transfer of Supercritical CO_2 in a Horizontal Channel by Lattice Boltzmann Method

Xiaodong Niu[1,*], Hiroshi Yamaguchi[1], Yuhiro Iwamoto[1], Xinrong Zhang[1,2], Mingjun Li[3] and Yuhiro Iwamoto[1]

[1] *Department of Mechanical Engineering, Doshisha University, Kyo-Tanabe-Shi, Kyoto 610-0321, Japan*
[2] *Department of Energy and Resources Engineering, College of Engineering, Peking University, Beijing 100871, P. R. China*
[3] *Department of Mechanical Engineering, Xiangtan University, Hunan 411105, P. R. China*

Abstract. The problem of forced convection heat transfer of supercritical CO_2 in a horizontal channel is investigated numerically by a lattice Boltzmann method. This study is stimulated by our recent experimental findings on solar collectors using supercritical CO_2 as a working fluid, which can achieve the collector efficiency high up to 70%. To deeply understand the heat transfer characteristics of supercritical CO_2 and provide a theoretical guidance for improving our current experimental system, in present study several typical experimental flow conditions are simulated. In particular, the work focuses on the convective heat transfer characteristics of supercritical CO_2 flowing in a horizontal channel with mediate Reynolds numbers ranging from 210 to 840 and constant heat fluxes from 400.0 to 800.0 W/m^2. The simulations show that the heat transfer increases with heat flux and decreases with Reynolds number. Furthermore, the mechanisms of heat transfer enhancement of supercritical CO_2 fluid are identified.

1 Introduction

Solar energy powered thermodynamic systems using supercritical CO_2 as a working

---

fluid have been proposed for combined generation of electrical power and thermal energy/refrigeration supplies [1,2]. Experimental studies [3,4] have been carried out to investigate supercritical CO_2-based cycle performance. Power generation efficiency is found to be 8.0%, comparable with that of solar cells and in addition, the cycle can also supply thermal energy/refrigeration to user. One of the major factors contributing to the high system efficiency is that the collector efficiency is surprisingly high, as found to be above 70.0%. The collector efficiency of 70.0% is much higher than that using water as the working fluid, in which case the maximum efficiency is only 50.0% [3–5]. In the experimental tests, all-glass evacuated solar collectors with a U-tube heat removal system are used and details of the collectors can be seen in references [2,3].
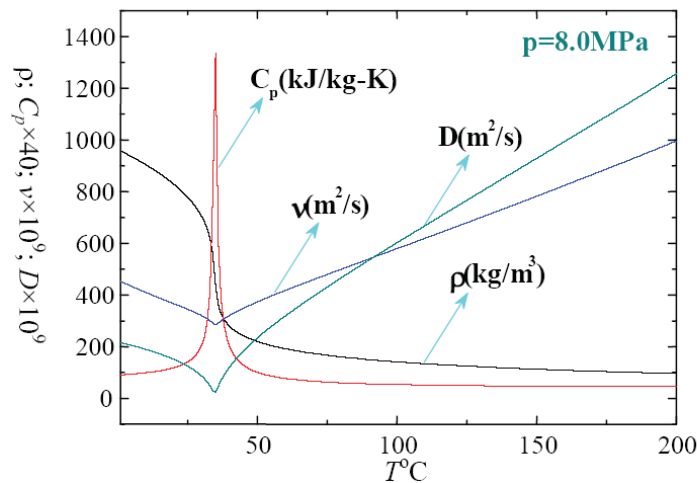

Figure 1: Thermophysical coefficients of CO_2 as functions of temperature.

However, the details and fundamental reasons for the enhanced convective heat transfer in a collector tube in the case of using supercritical CO_2 as the working fluid are still not very clear. This is because the behaviors of the thermophysical coefficients of CO_2, such as density, specific heat, viscosity and thermal diffusion are very complicated in the supercritical state. Fig. 1 shows variations of the CO_2 thermophysical coefficients of density ρ, specific heat C_p, kinematic viscosity v and thermal diffusion D as a function of temperature at the pressure of 8.0MPa. It is seen that the coefficients are very sensitive to the change of temperature. C_p achieves a sharp peak around 35°C and this is the pseudo-critical temperature for 8.0MPa; meanwhile, the two transport coefficients are minimal. The thermophysical properties are also influenced by the pressure. The striking dependence of thermophysical properties on both temperature and pressure would influence the flow and heat transfer characteristics.

As the first step towards a fundamental understanding and estimation of the heat transfer characteristics of supercritical CO_2 under forced convection conditions, in this paper, a lattice Boltzmann investigation of the supercritical CO_2 thermal flow in a simple geometrical configuration–a two-dimensional horizontal channel is carried out.

The lattice Boltzmann model (LBM) is based on that of Guo et al. [6], in which two particle distribution functions are used to describe the velocity and the temperature fields, respectively. Different from the model of Guo et al. using only temperature-dependent viscosity but constant thermal diffusivity to determine the relaxations of the particle collisions [6], the present LBM uses both temperature-dependent viscosity and thermal diffusion coefficients to calculate the particle relaxations so that the local information of flow field can be simulated.

The two-dimensional channel studied in the present work is based on the collector tube used in the experiment [3,4]. Particular interest is focused on the heat transfer characteristics with mass flow rates measured in the experimental tests within the range of the Reynolds number of 210 to 840. In the numerical model, the horizontal channel is heated at different constant heat fluxes being close to the values of solar radiations measured in the experiments. The present investigation mainly attempts to shed light on the convective heat transfer enhancement occurring in the experiments. In addition, the effects of the governing parameters such as Reynolds number and heat flux on the heat transfer problem under consideration are presented.

2 Lattice Boltzmann model

In mathematics, the hydrodynamics of supercritical CO_2 is described by the following equations

$$\partial_t \rho + \nabla \rho \mathbf{u} = 0, \tag{2.1a}$$

$$\partial_t \rho \mathbf{u} + \nabla \rho \mathbf{u} \mathbf{u} = -\nabla p + \eta \nabla^2 \mathbf{u}, \tag{2.1b}$$

$$\partial_t \rho T + \nabla \rho T \mathbf{u} = D \nabla^2 T, \tag{2.1c}$$

where t is the time, ρ, $\mathbf{u}$, p and T are density, velocity, pressure and temperature, respectively, η and D are dynamic viscosity and thermal diffusivity of fluid, respectively.

In the lattice Boltzmann frame, the above hydrodynamics can be solved by the following lattice Boltzmann equations [6]

$$f_\alpha(\mathbf{x} + \mathbf{e}_\alpha \delta t, t + \delta t) - f_\alpha(\mathbf{x}, t) = -\frac{1}{\tau_f}[f_\alpha(\mathbf{x}, t) - f_\alpha^{eq}(x, t)], \tag{2.2a}$$

$$g_\alpha(\mathbf{x} + \mathbf{e}_\alpha \delta t, t + \delta t) - g_\alpha(\mathbf{x}, t) = -\frac{1}{\tau_g}[g_\alpha(\mathbf{x}, t) - g_\alpha^{eq}(\mathbf{x}, t)], \tag{2.2b}$$

and the respective equilibrium distribution functions f_α^{eq} and g_α^{eq} are given by

$$f_\alpha^{eq}(\mathbf{x}, t) = w_\alpha \rho \left[1 + \frac{\mathbf{e}_\alpha \cdot \mathbf{u}}{c_s^2} + \frac{(\mathbf{e}_\alpha \cdot \mathbf{u})^2}{2c_s^4} - \frac{1}{2}\frac{\mathbf{u}^2}{c_s^2} \right], \tag{2.3a}$$

$$g_\alpha^{eq}(\mathbf{x}, t) = w_\alpha T \left[1 + \frac{\mathbf{e}_\alpha \cdot \mathbf{u}}{c_s^2} \right], \tag{2.3b}$$

where $\mathbf{x} = \mathbf{x}(x, y)$ is the spatial vector.

The weight coefficients w_α and the sound speed c_s are determined by the discrete velocity models and for the D2Q9 model they are

$$e_\alpha = \begin{cases} (0,0), \\ (\pm 1, 0), (0, \pm 1), \\ (\pm 1, \pm 1), \end{cases} \tag{2.4a}$$

$$w_\alpha = \begin{cases} \frac{4}{9}, & \alpha = 1, \\ \frac{1}{9}, & \alpha = 2, \cdots, 5, \\ \frac{1}{36}, & \alpha = 6, \cdots, 9, \end{cases} \tag{2.4b}$$

$$c_s^2 = \frac{1}{3}. \tag{2.4c}$$

The relaxation parameters τ_f and τ_g in Eqs. (2.2a) and (2.2b) are determined by the viscosity η and the diffusivity D, respectively, as

$$\tau_f = \frac{\eta}{\rho c_s^2 \delta t} + 0.5, \tag{2.5a}$$

$$\tau_g = \frac{D}{\rho c_s^2 \delta t} + 0.5. \tag{2.5b}$$

The density ρ, velocity $\mathbf{u}$ and temperature T are calculated by

$$\rho = \sum_{\alpha=1}^{9} f_\alpha, \qquad \mathbf{u} = \frac{1}{\rho} \sum_{\alpha=1}^{9} \mathbf{e}_\alpha f_\alpha, \qquad T = \sum_{\alpha=1}^{9} g_\alpha. \tag{2.6}$$

3   Problem defination and numerical simulations

We consider a horizontal channel as shown schematically in Fig. 2. The domain of interest is two-dimensional with dimensions of length L=200.0mm and height d=20.0mm. The computational geometry is bounded on the top and bottom by solid walls, which are assumed to be subjected to constant heat fluxes. The left and right surfaces are specified as inlet and outlet, respectively. We consider the case where the flow convection due to pump driving the supercritical CO_2 fluid. The flow is considered to be a developing flow with constant inlet velocity.

In numerical simulations, three inlet Reynolds numbers of Re_{in}=210, 420 and 840 and three constant heat flux conditions of q=400, 600 and 800[W/m] are investigated. In order to model accurately the solution variables with large gradients in the near-wall region and capture adequately the flow into and out of the channel, structured non-uniform grid systems are generated in the computational domain and the Taylor-series-expansion & least-square-based lattice Boltzmann scheme [8] is employed to solve the Eqs. (2.2a) and (2.2b). The grid is finer close to the wall, inlet and outlet (see Fig. 3). Grid independence of results is established by employing various grid
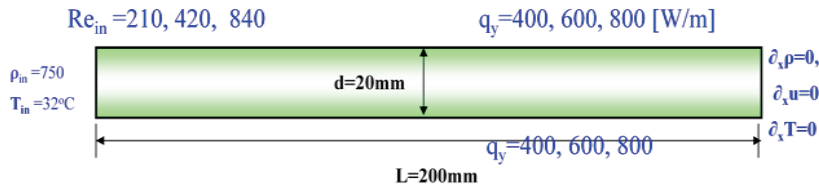
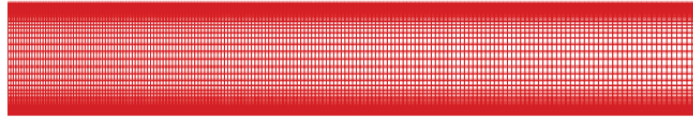Figure 2: Schematic diagram of forced convection problem of supercritical CO_2 flow in a horizontal channel.

Figure 3: Structured non-uniform grid of 61×1201.

resolutions, ranging from 31×601 to 121×2401. In the numerical study, a typical mesh of 61×1201 is used. Initially, the flow field is set stationary with constant inlet temperature. The boundary conditions for macroscopic quantities used in the simulations are depicted in Fig. 2. In the LBM implementation, non-equilibrium bounce back conditions of the distribution functions are applied on all the boundaries to mimic the non-slip and constant heat flux condition on the channel walls and constant and zero diffusion fluxes of physical quantities in the channel inlet and outlet, respectively. The thermophysical properties of supercritical CO_2 are the function of temperature and pressure and calculated by a Program Package for Thermo-physical Properties of Fluids database version 12.1 (PROPATH 12.1) [9].

The evaluations of the local heat transfer characteristics are based on the following local heat transfer coefficient h and Nusselt number Nu, respectively, as

$$Nu = \frac{hd}{\lambda_b}, \tag{3.1a}$$

$$h = \frac{\lambda_w}{T_w - T_b} \frac{\partial T}{\partial y}\bigg|_w, \tag{3.1b}$$

where T_b and λ_b are the bulk temperature and thermal conductivity and they are given by

$$T_b = \frac{\int_0^d \rho u T dy}{\int_0^d \rho u dy}, \qquad \lambda_b = \frac{\int_0^d \rho u \lambda dy}{\int_0^d \rho u dy}. \tag{3.2}$$

4 Results and discussions

Fig. 4 shows the typical velocity field of supercritical CO_2 flow in the channel at $Re_{in}=210$ and $q=400$. As shown in Fig. 4, it is seen that the flow quickly becomes fully developed flow after a very short entrance. One can also observe the velocity

Figure 4: Velocity field of developing supercritical CO_2 flow in the Channel at Re_{in}=210 and q=400.

boundary layer developed near the channel walls. Those observations are similar to the conventional fluid flows.

The variations of the thermophysical properties in the channel are important for understanding of mechanisms for heat transport. Thermophysical properties from the numerical prediction of the convective flow using supercritical CO_2 as working fluid were given using plots of steady-state condition. Fig. 5 presented distributions of thermal conductivity, specific heat and kinematic viscosity along the channel centerline at different Reynolds numbers and heat flux boundary conditions. To see the variation details of the thermo-physical properties inside the channel, we chose the specific heat as a representative and its distributions are displayed in Figs. 6 and 7 at constant Reynolds number and constant heat flux, respectively.

It can be clearly seen from Figs. 5-7 that the variation of the thermophysical properties of supercritical CO_2 was complicated, which makes the heat transfer of supercritical CO_2 very much different from conventional fluids. As shown in Figs. 5-7, the thermal conductivity, specific heat and viscosity changed not only along the channel, but also in the cross plane. Generally speaking, the thermophysical properties
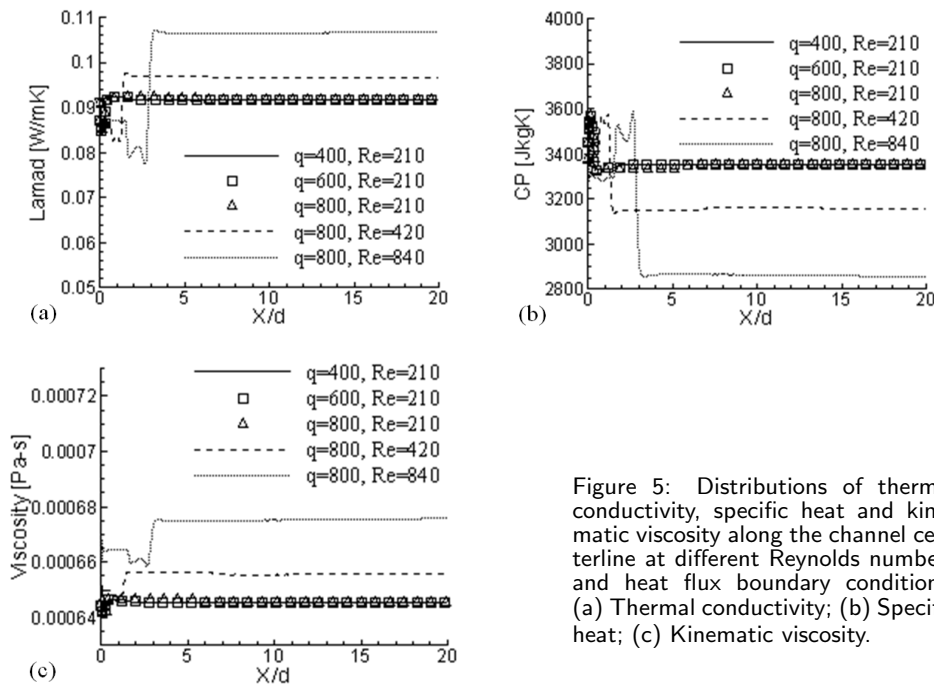

Figure 5: Distributions of thermal conductivity, specific heat and kinematic viscosity along the channel centerline at different Reynolds numbers and heat flux boundary conditions. (a) Thermal conductivity; (b) Specific heat; (c) Kinematic viscosity.
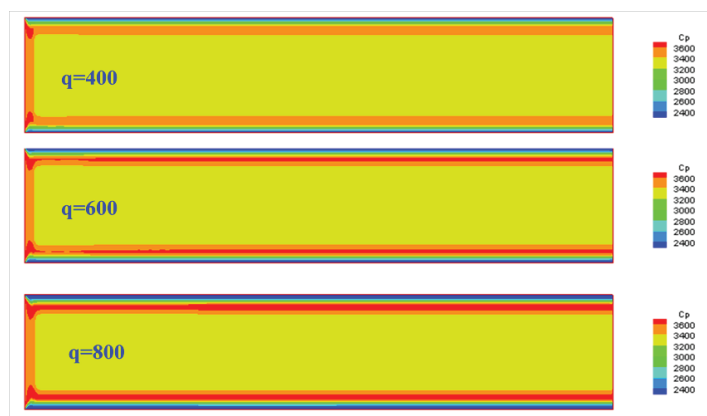
Figure 6: Distributions of specific heat inside the channel at $Re_{in}=210$ and heat flux boundary conditions.
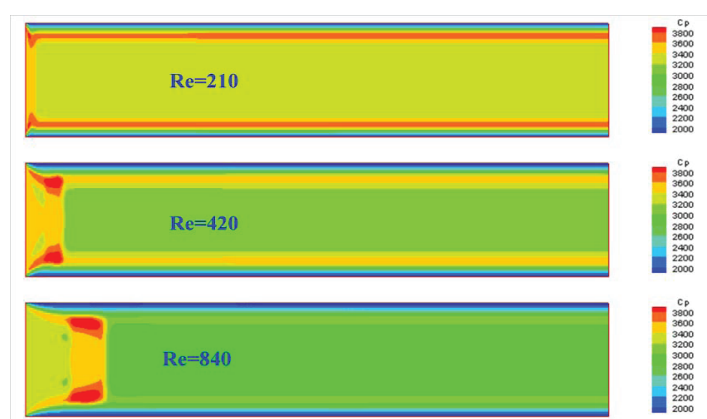

Figure 7: Distributions of specific heat inside the channel at three Reynolds numbers and $q=800[\text{W/m}]$.

vary drastically in the developing and boundary layer regions. Increasing heat flux has smaller effect on the distribution of the thermophysical properties than increasing Reynolds numbers. Reynolds number increase implies the inlet flow rate increases and as seen from Fig. 5, the thermal conductivity and kinematic viscosity are increased and the specific heat is decreased. Therefore, the inlet flow rate is significant on the performance of the heat transfer in the channel.

The heat transfer performance of supercritical CO_2 in the channel can be obtained by studying the local distributions of temperature, heat transfer rate and Nusselt numbers. Fig. 8 shows the distributions of temperature, heat transfer coefficient and Nusselt number along the channel at different Reynolds numbers and heat flux boundary conditions. Shown in Fig. 8, temperature along the channel centerline increases with both Reynolds number and heat flux. This is due to the high flow velocity giving faster heat convection than the low flow velocity and high heat flux meaning more heat input in a unit time.

Observed from Figs. 8(b) and (c), the changing of Reynolds number has small ef-
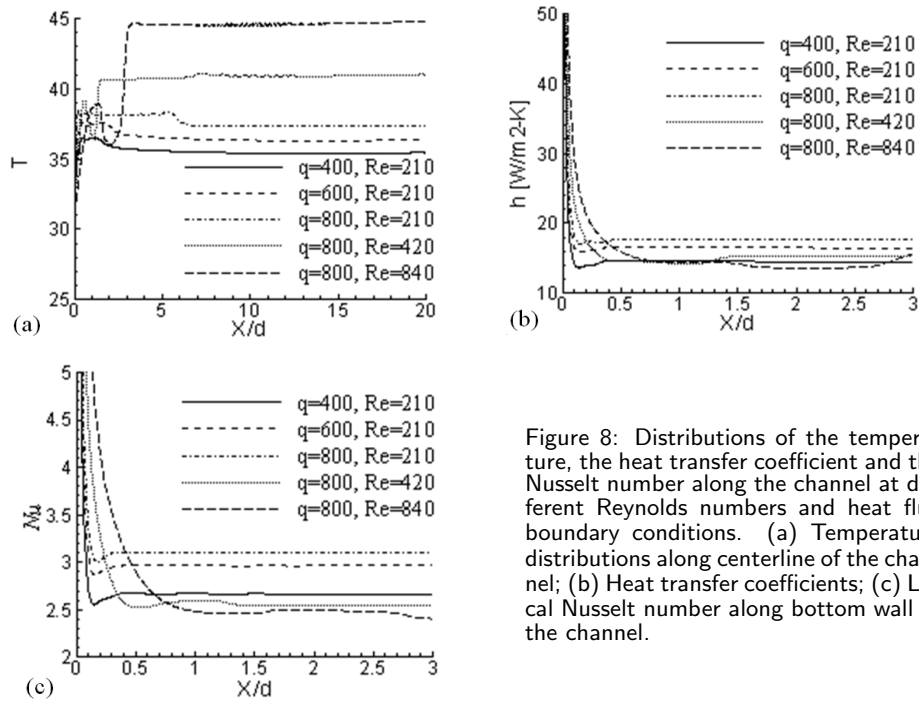
Figure 8: Distributions of the temperature, the heat transfer coefficient and the Nusselt number along the channel at different Reynolds numbers and heat flux boundary conditions. (a) Temperature distributions along centerline of the channel; (b) Heat transfer coefficients; (c) Local Nusselt number along bottom wall of the channel.

fect on the heat transfer coefficient and local Nusselt number comparing to the variation of heat flux. It is obvious that the heat flux increasing results in increase of the heat transfer coefficient and Nusselt number, suggesting the heat transfer is en-

Figure 9: Distributions of temperature inside the channel at Re_{in}=210 and heat flux boundary conditions.

Figure 10: Distributions of temperature inside the channel at three Reynolds numbers and q=800[W/m].

hanced. However, increasing Reynolds number decreases these two parameters. This is because Reynolds number increasing causes the temperature distribution more homogenous and thus the temperature gradient near the wall decreases. These can be seen from Figs. 9 and 10. The temperature gradient near the wall increases with heat flux increasing and decreases with increase of the Reynolds number.

5   Conclusions

The problem of low Reynolds number forced convection of supercritical CO_2 in a horizontal channel is studied numerically by a lattice Boltzmann method. The results show that the heat transfer increases with the heat flux and decreases with the Reynolds number in the present study. Furthermore, the mechanisms of heat transfer enhancement of supercritical CO_2 are investigated. The temperature gradient near the wall increases with heat flux increasing and decreases with increase of the Reynolds number.

References

[1] X. R. ZHANG, H. YAMAGUCHI, K. FUJIMA, M. ENOMOTO AND N. SAWADA, *A feasibility study of CO_2-based Rankine cycle powered by solar energy*, JSME. Int. J., Ser. B., 48 (2005), pp. 540–547.

[2] H. YAMAGUCHI, X. R. ZHANG, K. FUJIMA, M. ENOMOTO AND N. SAWADA, *A solar energy powered Rankine cycle using supercritical carbon dioxide*, Appl. Therm. Eng., 26 (2006), pp. 2345–2354.

[3] X. R. ZHANG, H. YAMAGUCHI, K. FUJIMA, M. ENOMOTO AND N. SAWADA, *Study of solar energy powered transcritical cycle using supercritical carbon dioxide*, Int. J. Energy. Res., 30 (2006), pp. 1117–1129.

[4] X. R. ZHANG, H. YAMAGUCHI, K. FUJIMA, M. ENOMOTO AND N. SAWADA, *Experimental performance of solar powered system using carbon dioxide*, AIP Conference Proceedings, 832 (2006), pp. 419–424.

[5] X. R. ZHANG, H. YAMAGUCHI, K. FUJIMA, M. ENOMOTO AND N. SAWADA, *Theoretical analysis of a thermodynamic cycle powered by solar energy for power and heat generation using supercritical carbon dioxide*, The 18th International Conference on Efficiency, Cost, Optimization, Simulation and Environmental Impact of Energy Systems (ECOS 2005), Trondheim, Norway, pp. 1641–1648.

[6] Z. GUO AND T. S. ZHAO, *Lattice Boltzmann simulation of natural convection with temperature-dependent viscosity in a porous cavity*, Prog. Comput. Fluid. Dyn., 5 (2005), pp. 110–117.

[7] C. SHU, Y. T. CHEW AND X. D. NIU, *Least-squares-based lattice Boltzmann method: a meshless approach for simulation of flows with complex geometry*, Phys. Rew. E., 64 (2001), 045701.

[8] D. A. WOLF-GLADROW, Lattice-Gas Cellula Automata and Lattice Boltzmann Models, Springer, Berlin, 2000.

[9] PROPATH GROUP, PROPATH V12.1, 2001.